Pharm Res (2012) 29:3143–3155
DOI 10.1007/s11095-012-0807-4

RESEARCH PAPER

Novel Comb-Shaped PEG Modification Enhances the Osteoclastic Inhibitory Effect and Bone Delivery of Osteoprotegerin After Intravenous Administration in Ovariectomized Rats

Yoshihiro Miyaji • Yuji Kasuya • Yoshitake Furuta • Atsushi Kurihara • Masayuki Takahashi • Ken-ichi Ogawara • Takashi Izumi • Osamu Okazaki • Kazutaka Higaki

Received: 10 February 2012 / Accepted: 8 June 2012 / Published online: 23 June 2012

ABSTRACT

Purpose Recombinant osteoprotegerin (OPG) has been proven to be useful for treating various bone disorders such as osteoporosis. To improve its *in vivo* pharmacological effect, OPG was conjugated to novel comb-shaped co-polymers of polyethylene glycol (PEG) allylmethylether and maleamic acid (poly(PEG), 5 kDa). Biodistribution and bioactivity were evaluated.

Methods OPG was conjugated *via* lysine to poly(PEG) and to linear PEG (0.5 kDa and 5 kDa). Poly(PEG)-OPG was compared with linear PEG0.5k-OPG and PEG5k-OPG in terms of *in vitro* and *in vivo* efficacy and bone distribution.

Results The *in vitro* receptor binding study showed that poly (PEG)-OPG could be the most bioactive among the three PEG-OPG derivatives. Pharmacokinetic studies in ovariectomized (OVX) rats showed that serum half-life and AUC of poly(PEG)-OPG were comparable with those of linear PEG-OPG derivatives. For *in vivo* pharmacological effect, poly(PEG)-OPG showed the strongest inhibitory effect on bone resorption activity in OVX rats. Poly (PEG)-OPG demonstrated enhanced bone marrow distribution with higher selectivity than linear PEG5k-OPG.

Conclusion Poly(PEG) modification could provide longer residence time in serum and higher bone-marrow specific delivery of OPG, leading to a higher *in vivo* pharmacological effect.

KEY WORDS accelerator mass spectrometry · bone marrow distribution · drug delivery · osteoporosis · PEGylation

INTRODUCTION

Osteoprotegerin (OPG) is a member of the tumor necrosis factor receptor (TNFR) superfamily (1,2) and a heparin-binding basic glycoprotein with an apparent molecular weight (M_w) of 110 kDa as a homodimer (1,3). OPG acts as a soluble secreted receptor for the receptor activator of nuclear factor-kappaB ligand (RANKL) expressed on the osteoblasts, and prevents it from activating the receptor activator of nuclear factor-kappaB (RANK) on the osteoclast surface (4–7). OPG was found to increase bone density and strength and to improve the bone turnover state, which can lead to an effective treatment of various bone disorders such as osteoporosis and rheumatoid arthritis (1,8–11). However, frequent administration at high doses of OPG was required to exert the *in vivo* pharmacological effect because OPG was rapidly and predominantly distributed to the liver after systemic administration (12).

Y. Miyaji • Y. Furuta • A. Kurihara • M. Takahashi • T. Izumi • O. Okazaki
Drug Metabolism and Pharmacokinetics
Research Laboratories, Daiichi Sankyo Co., Ltd.
1-2-58 Hiromachi, Shinagawa-ku
Tokyo 140-8710, Japan

Y. Kasuya
Lead Discovery and Optimization
Research Laboratories I, Daiichi Sankyo Co., Ltd.
1-2-58 Hiromachi, Shinagawa-ku
Tokyo 140-8710, Japan

K.-i. Ogawara • K. Higaki
Department of Pharmaceutics, Faculty of Pharmaceutical Sciences
Okayama University
1-1-1 Tsushima-naka, Kita-ku
Okayama 700-8530, Japan

Present Address:
Y. Miyaji (✉)
Center for Pharmaceutical and Biomedical Analysis
Daiichi Sankyo RD Novare Co., Ltd.
1-16-13 Kitakasai, Edogawa-ku
Tokyo 134-8630, Japan
e-mail: miyaji.yoshihiro.gw@rdn.daiichisankyo.co.jp

Bioactive proteins intended for diagnosis and treatment are required to ideally possess enhanced target tissue exposure with retained biological activity. Modification of proteins by attaching polyethylene glycol (PEG) chains (PEGylation) has been commonly used to improve molecular stability (13,14), to reduce immunogenicity (15) and to prolong the residence time in blood circulation (16–18). Many researchers have shown that PEGylation is a well-established strategy for intensifying the therapeutic and biotechnological properties of proteins (19,20). The ε-amino group of lysine and the α-amino group of the N-terminal residue are most commonly used as reactive sites on proteins for PEGylation. Thus, most PEGylation methods usually result in modification of multiple sites, which might lead to reduction of *in vitro* biological activity and receptor binding affinity of proteins because the biological active site might also be covered due to steric hindrance of PEG (19). Such a low receptor binding affinity caused by PEGylation could be overcompensated by the systemic exposure increased by PEGylation, resulting in the enhancement of *in vivo* pharmacological efficacy (17). However, it is still a challenging technique for achieving both the enhancement of the target tissue exposure and retention of receptor binding affinity. A PEGylated interferon alpha-2 (PEG-IFN-α2), PEGASYS (Roche), achieves a superior prolonged half-life and slight *in vitro* biological activity compared with that of the unmodified protein (21). In contrast, PEG-Intron (Schering Corporation), another PEG-IFN-α2, has a moderately improved half-life whereas it possesses relatively retained biological activity of the original protein (22). Thus, depending on the therapeutic strategies, appropriate PEGylation conditions are required to achieve an optimal balance between the reduced biological activity and the prolonged *in vivo* half-lives.

Recently, our group developed novel comb-shaped copolymers of polyethylene glycol allylmethylether and maleamic acid (poly(PEG)) as a protein modifier (23). Our poly(PEG) has multivalent and mild reactive sites of maleamic acid, which has a different structure and characteristics from the comb-shaped PEGs reported previously (24,25), and comprises of linear PEG chains with an M_w of 0.5 kDa. Our previous study demonstrated that the modification of OPG with the poly(PEG) increased the systemic exposure, resulting in its expanded pharmacological ability to increase bone density compared with that of unmodified OPG (23). However, the advantage of poly(PEG) over commonly-used linear PEG remains unknown in terms of ability to retain the receptor binding affinity of OPG, and to enhance *in vivo* pharmacological activity and the bone tissue distribution.

In the present study, two different strategies of PEGylation for the conjugation of recombinant human OPG were employed as follows: [1] random PEGylation of primary amines using comb-shaped poly(PEG) with a total M_w of 5 kDa (poly(PEG)-OPG); [2] random PEGylation of primary amines using N-hydroxysuccinimide derivatives of linear monomethoxy PEG (mPEG-NHS) with different M_w (0.5 kDa or 5 kDa). Since PEG size can affect the pharmacokinetic properties and the biological activities of PEGylated proteins (14,26,27) and poly(PEG) is a comb-Shaped PEG (total M_w ca. 5 kDa) having linear 0.5 kDa PEG chains, two kinds of linear PEG with M_w of 0.5 kDa and 5 kDa were used to synthesize the linear PEG-OPG derivatives. Then, the *in vitro* receptor binding affinity, *in vivo* pharmacological efficacy, target tissue distribution and its distribution mechanism of poly(PEG)-OPG were evaluated and compared with those of linear PEG-OPG derivatives by utilizing ovariectomized rats as an osteoporotic rat model (28).

MATERIAL AND METHODS

Reagents

Recombinant human osteoprotegerin (OPG) was produced by Daiichi Sankyo Co., Ltd. (Tokyo, Japan). AM-0510K (polyPEG500-MAn(5 k)) and ^{14}C-labeled AM-0510K (total molecular weight (M_w), ca. 5 kDa; M_w of monomethoxy polyethylene glycol chain, ca. 0.5 kDa), the precursor of poly (PEG), were purchased from NOF Corporation (Tokyo, Japan) and Sekisui Medical Co., Ltd. (Tokyo, Japan), respectively. Non-radiolabeled and ^{14}C-labeled poly(PEG) were synthesized from AM-0510K as previously described except that AM-0510K was stirred in 28% of aqueous ammonia at 15°C for 20 h (23). The chemical structures of AM-0510K and poly(PEG) and their ^{14}C-labeled positions are shown in Fig. 1a. N-hydroxysuccinimide (NHS) derivatives of linear monomethoxy PEG (mPEG-NHS) with M_w of 0.5 kDa (MS $(PEG)_8$) and 5 kDa (SUNBRIGHT ME-050AS) were purchased from Thermo Fisher Scientific Inc. (Waltham, MA) and NOF Corporation, respectively. A 96 well plate precoated with anti-glutathione-S-transferase (GST) antibody was purchased from Thermo Fisher Scientific Inc. The protein concentrations of OPG and PEGylated OPG derivatives were determined using a DC protein assay kit (Bio-Rad Laboratories, Inc., Hercules, CA) with bovine serum albumin as a protein standard. Other reagents and solvents used were commercially available.

Synthesis of Poly(PEG)-OPG and Linear PEG-OPG Derivatives

To synthesize poly(PEG)-OPG, non-radiolabeled or ^{14}C-labeled poly(PEG) were attached to the lysine residues in OPG by the method as previously reported with slight

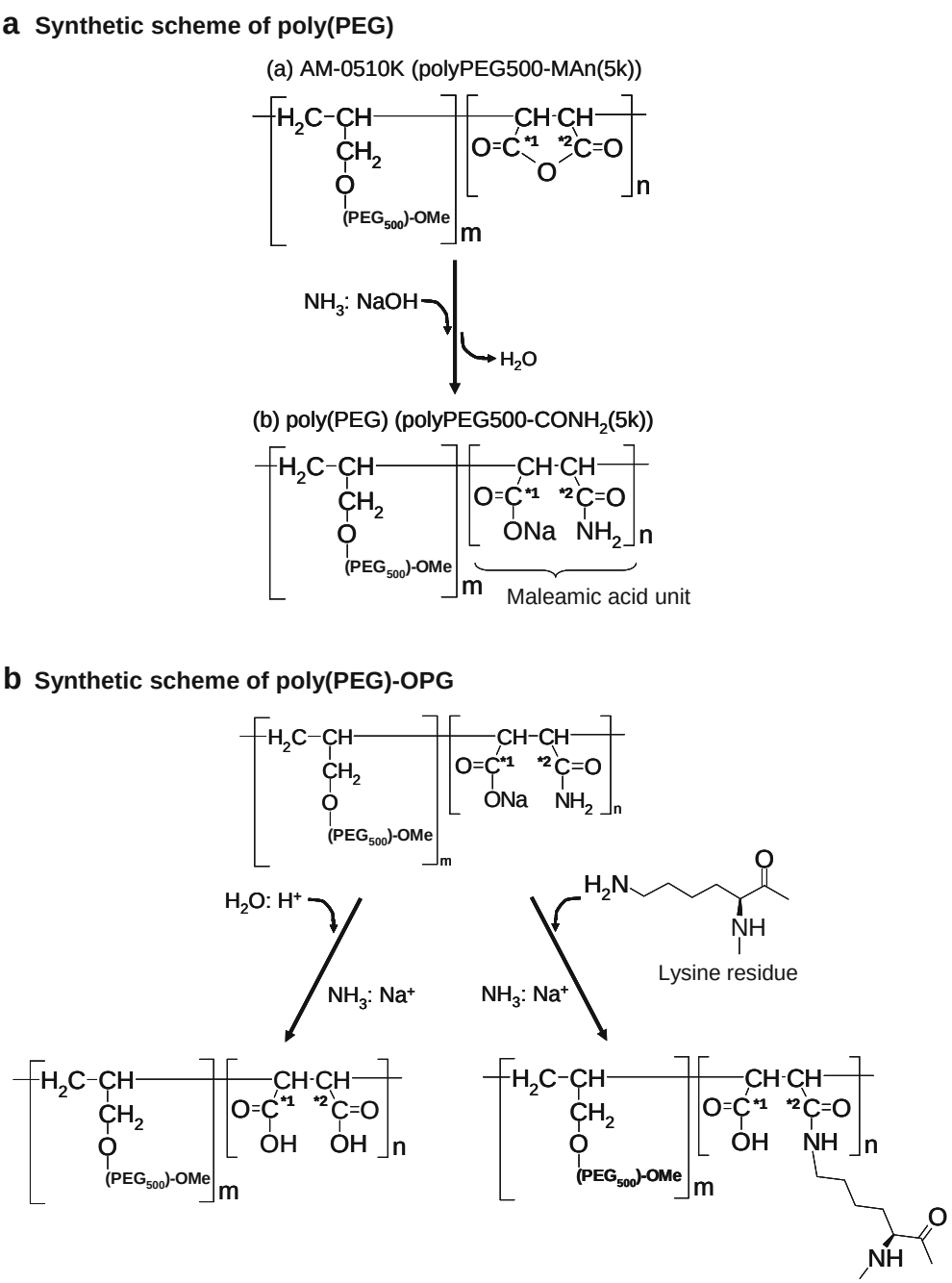

Fig. 1 Synthetic scheme of (**a**) poly(PEG) and (**b**) poly(PEG)-OPG. Chemical structure of (**a**) AM-0510K and (**b**) comb-shaped poly(PEG) molecule. The asterisk in the structure denotes the position labeled with ^{14}C.

modification (23). The supposed synthetic scheme of poly (PEG)-OPG and the ^{14}C-labeled position are shown in Fig. 1b. Briefly, poly(PEG) was added to the OPG solution in a phosphate buffer (100 mM phosphate buffer, 150 mM NaCl, pH6.0) at a molar ratio of 30 (modifier/OPG). The pH of the mixture was adjusted to 4.7 and incubated at 37°C for 96 h. Although all maleamic acids of poly(PEG) could be hydrolyzed by water after 96-h incubation at 37°C, pH4.7, the conjugation ratio of poly(PEG)-OPG could not be decreased under these conditions during the incubation. For synthesis of linear PEG-OPG derivatives, PEG0.5k-OPG and PEG5k-OPG, OPG (5 mg/ml in 10 mM phosphate buffer, 150 mM NaCl, pH8.0, 0.1% polysorbate 80) was conjugated with more than 50-fold molar linear m-PEG-NHS with PEG M_w of 0.5 kDa and 5 kDa, respectively, at room temperature for 1 h. PEG-OPG derivatives were purified using a gel-filtration column, Superdex 200 HiLoad 16/60 (GE Healthcare UK Ltd., Little Chalfont, UK) at 4°C. Isocratic elution was carried out at a flow rate of 1.2 ml/min using PBS (10 mM phosphate buffer, 150 mM NaCl, pH7.4). The fractions of PEG-OPG derivatives were collected by monitoring the eluate at 220 nm, and then concentrated at 4°C using an ultrafiltration (Amicon Ultra NMWL:50 K, Millipore, Billerica, MA). The radiochemical purity of ^{14}C-poly(PEG)-OPG was determined to be over

97%. The concentrated PEG-OPG derivatives were stored at −80°C until use. The purified PEG-OPG derivatives were analyzed by sodium dodecyl sulfate-polyacrylamide gel (7.5%, Ready gel J, Bio-Rad Laboratories) electrophoresis (SDS-PAGE), conducted at a constant voltage of 200 V. Gels were then fixed and stained for protein using Coomassie Blue R-250 (Bio-Rad Laboratories). The apparent M_w of PEGylated OPG derivatives were determined by KODAK 1D Image Analysis Software (Eastman Kodak Company, Rochester, NY).

Radioiodination of OPG, Poly(PEG)-OPG and PEG5k-OPG

OPG, poly(PEG)-OPG and PEG5k-OPG (50 μg) were labeled with 1 mCi of sodium ^{125}I-iodide (PerkinElmer, Inc., Waltham, MA) using a modified lactoperoxidase method as previously described (12). Briefly, to OPGs dissolved in PBS-T0.01 (PBS containing 0.01% polysorbate 80, pH7.4) supplemented with 74 μg/ml lactoperoxidase (Sigma-Aldrich Corp., St. Louis, MO), 10 μL of hydrogen peroxide (0.88 mM) was added, and then hydrogen peroxide was added three times at 5 min intervals. The protein-associated radioactivity was separated from the free ^{125}I-idodine using a PD-10 column (GE Healthcare UK Ltd.) and the radiochemical purity was determined to be over 97%. The radioactivity in the samples was determined by gamma counting for 1 min using an Auto-Gamma Counting Systems RiaStar (PerkinElmer, Inc.).

In Vitro Receptor Binding Affinities of OPG and PEG-OPG Derivatives

The inhibitory effect of OPG and PEG-OPG derivatives on the receptor binding of ^{125}I-OPG was determined using the cell-free binding assay (5,12) with minor modification. Briefly, human RANKL fused to GST (Oriental Yeast Co., Ltd., Tokyo, Japan) was added to each well of a 96-well plate precoated with anti-GST antibody and then incubated at room temperature for 2 h. After washing with PBS-T0.1 (PBS containing 0.1% polysorbate 20, pH7.4), the well was incubated with ^{125}I-OPG (final concentration, 0.03 nM) and OPG or PEG-OPG derivatives in total volume of 100 μl of PBS-T0.1 at room temperature for 2 h. After collecting the supernatant, each well was washed with PBS-T0.1 and lyzed with 100 μl of 2 N NaOH. Radioactivity in the supernatant for free OPGs and the lysate for bound OPGs was determined by gamma counting. Non-specific binding of ^{125}I-OPG was also evaluated in the presence of 50-fold excess of non-labeled OPG and was subtracted from each bound amount. The bound levels of ^{125}I-OPG to RANKL were expressed as the percentage of the control level, which was determined by incubation with only ^{125}I-OPG. The half-maximum inhibition concentration (IC_{50}) of OPG or PEG-OPG derivatives was obtained by using the following equation:

$$B = B_0 - \frac{B_{\max} \cdot C}{IC_{50} + C} \quad (1)$$

with WinNonlin Professional (Version 5.2.1, Pharsight Corporation, Mountain View, CA). In the equation, B, B_0 and B_{max} mean the binding percent, the total binding percent (=100%) and maximum binding percent, respectively.

Animals

Female Fischer (F344) rats, ovariectomized (OVX) at 12 week of age, were purchased from Charles River Japan, Inc. (Yokohama, Japan). OVX rats were acclimatized for 2 week in a controlled animal area at a room temperature of 23±2°C under a 12-h light-dark cycle with artificial lighting. Rats were fasted overnight before the experiments and a laboratory diet was given to them 8 h after each administration. Tap water was given *ad libitum* throughout the study. Animal experiments were conducted in accordance with the Institutional Animal Care and Use Committee of Daiichi Sankyo Co., Ltd.

Pharmacokinetic Studies

OPG, PEG0.5k-OPG, PEG5k-OPG (0.3 mg/2 ml/kg) or poly(PEG)-OPG (0.5 μg/2 ml/kg and 0.3 mg/2 ml/kg), dissolved in PBS-T0.01, was intravenously administered to OVX rats (n=4) under ether anesthesia. Serum concentrations of each protein were determined using Human Osteoprotegerin Instant ELISA kit (eBioscience Inc., San Diego, CA). Pharmacokinetic parameters for each protein were determined using WinNonlin Professional. The area under the serum concentration-time curve (AUC) extrapolated to infinity was calculated following the trapezoidal rule. The elimination terminal half-life, the total body clearance (CL), the mean residence time (MRT) and the volume of distribution at steady state (Vdss) were calculated.

For the tissue distribution study, OVX rats (n=3) were sacrificed at 3, 24 and 168 h after intravenous administration of ^{14}C-poly(PEG)-OPG (0.5 μg/kg, 1.4 nCi/kg) with or without co-administration of non-radiolabeled poly(PEG)-OPG (0.3 mg/kg). Blood was withdrawn from the abdominal aorta. The liver, kidneys, spleen, muscle, femur bones and bone marrow were excised, rinsed with PBS (pH7.4), and weighed. Then the radioactivity in each tissue and serum was determined using accelerator mass spectrometry (AMS) as described below. The radioactivity of the dosing solution was measured by liquid scintillation counting using a 2300TR counter (PerkinElmer, Inc.). For analysis of the metabolite profile, the serum and bone marrow were

collected at 3 h after intravenous dosing of ^{14}C-poly(PEG)-OPG (0.5 μg/kg) into OVX rats. The bone marrow was hydrolyzed with an equivalent amount of lysis buffer (PBS-T0.01, pH7.4, 2% Triton-X and protease inhibitor cocktail (Sigma-Aldrich)) on ice for 1 h and then homogenized. The mixture was centrifuged at 12,000*g*, 4°C for 3 min, and the supernatant was subjected to the HPLC system. The serum sample was mixed with an equal volume of lysis buffer and the obtained sample was used for HPLC analysis.

Pharmacological Study

After intravenous administration of OPG or PEG-OPG derivatives (0.3 mg/kg) to OVX rats (n=5), blood samples were collected from the jugular vein at 0, 2, 5 and 10 day post-dose. Serum osteoclast-derived tartrate-resistant acid phosphatase form 5b (TRACP 5b) levels were determined as a biomarker of histological determination for the osteoclast number and bone resorption activity in rat bone (29), using a RatTRAP Assay kit (Immunodiagnostic Systems Ltd., Tyne & Wear, UK). The serum TRACP 5b levels were expressed as a percentage of the level at Day 0 (% of initial) in each treatment group. The AUC values of the serum TRACP 5b levels were also calculated using the trapezoidal rule.

Accelerator Mass Spectrometry (AMS) Analysis of Total ^{14}C Content in the Tissues

AMS analysis was performed at the Institute of Accelerator Analysis Ltd. (Motomiya, Japan). Sample preparation for AMS analysis was performed according to the method described by Kitagawa *et al.* (30) and Miyaji *et al.* (31). To convert to units of the ^{14}C-concentration (dpm ^{14}C/g or ml) in the sample, the percentage of carbon is accounted for as follows:

$$(\mathrm{dpm/g\,or\,mL}) = \left(\mathrm{dpm}^{14}\mathrm{C/gC}\right) \times \mathrm{Carbon\,content(gC/g\,or\,ml)}$$

where the carbon content (gC/g or ml) in the sample was calculated from the amount of CO_2 gas measured with a capacitance gauge. The ^{14}C-content in the samples was expressed by the following equation:

$$\begin{aligned}\mathrm{Sample}^{14}\mathrm{C\text{-}content} &= \mathrm{compound}^{14}\mathrm{C\text{-}content} \\ &+ \mathrm{biological}^{14}\mathrm{C\text{-}content} \\ &+ \mathrm{carrier}^{14}\mathrm{C\text{-}content}\end{aligned}$$

The biological ^{14}C-content was obtained from the pre-dose sample in each matrix, and the carrier ^{14}C-content was measured independently. The compound ^{14}C-content was calculated by subtracting these two values from the total ^{14}C-content in the sample.

HPLC Analysis

^{14}C-poly(PEG)-OPG standard solution was analyzed by size exclusion (SE)-HPLC using a Shimadzu LC-10Avp HPLC system (Kyoto, Japan) with an online radioactivity detector (β-RAM model 3, IN/US Systems, Tampa, FL). An aliquot of ^{14}C-poly(PEG)-OPG was injected on to a 300×7.8 mm TSKgel GW3000SWXL column (TOSOH Co., Ltd., Tokyo, Japan) at room temperature. Elution was carried out using PBS-T0.01 at a flow rate of 1 ml/min and mixed with Ecoscint Flow (National Diagnostics, Atlanta, GA), a scintillation fluid cocktail, at a flow rate of 1 ml/min. For analysis of the metabolite profile of ^{14}C-poly(PEG)-OPG, the serum and bone marrow samples were separated by HPLC, the eluate was fractionated at a 1 min interval and the ^{14}C-content in each fraction was determined by AMS as described above.

Whole-Body Autoradioluminography and Imaging Analysis

At 3 h after intravenous administration of ^{125}I-PEG5k-OPG or ^{125}I-poly(PEG)-OPG (0.5 μg/6 μCi/kg) to OVX rats (n=3), blood samples were collected and the rats were euthanized with CO_2 and then fixed by flash-freezing in an n-hexane/dry ice bath and embedded in 5% carboxymethyl cellulose. Fifty-μm thick sagittal cryosections for whole-body autoradioluminography were prepared as previously described (12). The sections were each exposed to an imaging plate (BAS-MS2040, Fuji Photo Film Co., Ltd.; Tokyo, Japan) for 24 h. The imaging plates were then analyzed using a Bio Imaging Analyzer (BAS-2500, Fuji Photo Film Co., Ltd.). The intensity of the radioactivity (photo-stimulated luminescence per unit area, PSL/mm^2) was determined for each tissue. The radioactivity in the blood (cpm/g) and the dosing solution was determined by gamma counting. Each calibration curve was prepared from the PSL/mm^2 value of the blood sample enclosing the known radioactivity concentration (cpm/g) obtained from each rat. The PSL/mm^2 value in each tissue was converted to the radioactivity in each tissue (cpm/g) using the calibration curve.

Statistical Analysis

All data were expressed as the mean ± S.D. of more than three experiments. The statistical analysis was performed using SAS System Release 8.2 (SAS Institute Inc., Cary, NC). The statistical significance in the differences of the means was evaluated by Student's t-test and Tukey's test for the single and multiple comparisons of experiment groups, respectively. Differences were considered to be significant when $p<0.05$.

RESULTS

Physicochemical Characteristics

The apparent M_w of OPG, poly(PEG)-OPG, and the two different linear PEG-OPG derivatives (PEG0.5k-OPG and PEG5k-OPG) analyzed by SDS-PAGE were 90 kDa, 110 kDa, 130 kDa and 240 kDa, respectively (Fig. 2). The apparent M_w of OPG obtained in the present study was slightly different from the reported values (1,3). This was thought to be due to the difference in the acrylamide concentrations of gels used for SDS-PAGE. The specific radioactivity of ^{14}C-poly(PEG) and ^{14}C-poly(PEG)-OPG was estimated to be 4.26 Bq per pmol of ^{14}C-polyPEG and 9.7 Bq per pmol of OPG using the apparent M_w of ^{14}C-poly(PEG) (5 kDa) and OPG (90 kDa), respectively. From the ratio of the specific radioactivity of ^{14}C-poly(PEG)-OPG to that of ^{14}C-poly(PEG), the average number of ^{14}C-poly(PEG) molecules attached to an OPG molecule was estimated to be approximately 2.28. The attached number of poly(PEG) was also estimated to be about 4 based on the calculation by dividing the M_w difference (ca. 20 kDa) between poly(PEG)-OPG and OPG by the M_w of poly(PEG) (ca. 5 kDa). In a similar manner, the number of linear PEG0.5k or PEG5k molecules attached to OPG could be estimated to be approximately 80 or 30, respectively.

Receptor Binding Affinity

The *in vitro* receptor binding affinities of OPG, poly(PEG)-OPG, PEG0.5k-OPG and PEG5k-OPG were determined in the cell-free inhibition assay against the binding of ^{125}I-OPG to RANKL (Fig. 3). OPG was found to have the highest affinity for its receptor with an IC_{50} value of 0.215 ± 0.048 nM. On the other hand, the IC_{50} of poly(PEG)-OPG was 0.437 ± 0.186 nM, indicating that poly(PEG)-OPG retains high affinity for the receptor comparable with that of unmodified OPG. Furthermore, it was also found that the affinity of poly(PEG)-OPG was >1000-fold and 6-fold greater than those of PEG0.5k-OPG and PEG5k-OPG, respectively (Fig. 3).

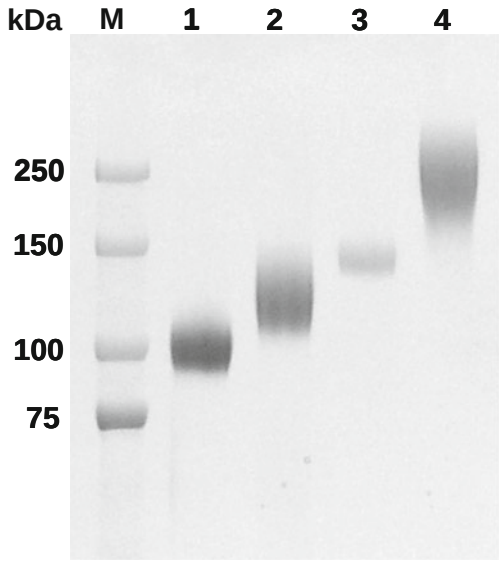

Fig. 2 SDS-PAGE analysis of OPG and PEG-OPG derivatives. Lane M, molecular weight marker; lane 1, OPG; lane 2, poly(PEG)-OPG; lane 3, PEG0.5k-OPG; lane 4, PEG5k-OPG. Gels were stained with Coomassie blue.

Pharmacokinetic Profiles in OVX Rats

Serum concentration-time profiles of OPG, poly(PEG)-OPG, PEG0.5k-OPG and PEG5k-OPG (0.3 mg/kg) after intravenous administration to OVX rats are shown in Fig. 4. Pharmacokinetic parameters are summarized in Table I. Unmodified OPG was rapidly eliminated from the systemic circulation with a half-life of 2.54 h at the terminal phase, whereas poly(PEG)-OPG, PEG0.5k-OPG and PEG5k-OPG had significantly prolonged terminal half-lives of 10.5, 14.6 and 11.6 h, respectively. The AUC values of PEG-OPG derivatives were more than 90 times larger than that of unmodified OPG, especially poly(PEG)-OPG and PEG0.5k-OPG showed the largest values. The results also showed that CL and Vdss were significantly decreased by PEGylation.

In Vivo Pharmacological Effect in OVX Rats

The *in vivo* pharmacological activities of OPG, poly(PEG)-OPG, PEG0.5k-OPG and PEG5k-OPG (0.3 mg/kg) were evaluated in OVX rats by observing their decreasing effect on the serum TRACP 5b level, a biomarker of histological determination of osteoclast bone resorption activity (Fig. 5). In poly(PEG)-OPG- and PEG5k-OPG-treated rats, serum levels of TRACP 5b reached the minimal levels on Day 2, then gradually increased to the same level as those in OPG- and PEG0.5 k-OPG-treated rats on Day 10. Single administration of poly(PEG)-OPG or PEG5k-OPG significantly decreased the serum levels of TRACP 5b on Day 2 to 37% and 59% of the OPG value, respectively. Furthermore, poly(PEG)-OPG demonstrated significantly the most effective pharmacological action among all the preparations examined.

Tissue Distribution of ^{14}C-poly(PEG)-OPG

Figure 6 shows the time course of the total radioactivity in the tissues after intravenous administration of ^{14}C-poly(PEG)-OPG at a tracer dose (0.5 μg/kg) to OVX rats. The radioactivity was cleared from the circulation relatively fast, but the distribution of radioactivity to the bone marrow (14.1% of dose/g tissue) was very fast and reached the highest level among the tissues examined. The high levels of radioactivity were also observed in the liver (9.63% of dose/g tissue) and spleen (7.54% of dose/g tissue) at 3 h post-dose. The levels of

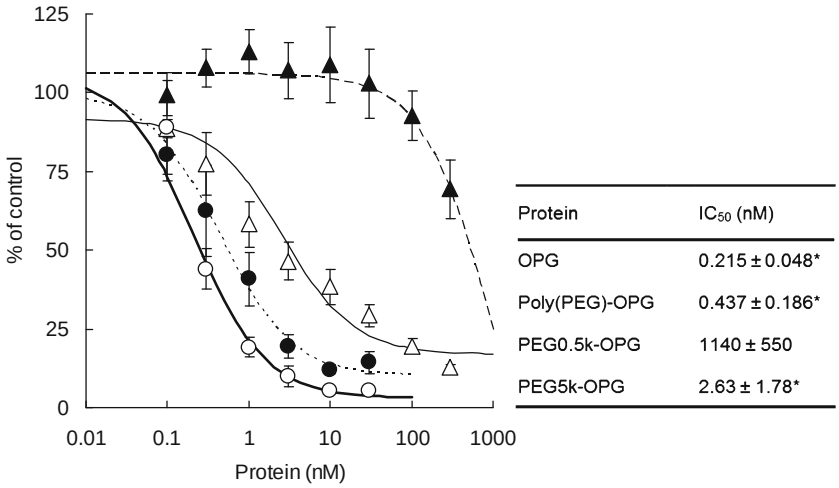

Protein	IC_{50} (nM)
OPG	0.215 ± 0.048*
Poly(PEG)-OPG	0.437 ± 0.186*
PEG0.5k-OPG	1140 ± 550
PEG5k-OPG	2.63 ± 1.78*

Fig. 3 *In vitro* receptor binding affinities of OPG and PEG-OPG derivatives to RANKL. The inhibitory effects of OPG (*open circle*), poly(PEG)-OPG (closed circle), PEG0.5k-OPG (*closed triangle*) and PEG5k-OPG (*open triangle*) were determined in the cell-free inhibition assay against binding of ^{125}I-OPG to RANKL. The data were fitted to Eq. 1 and the lines shows the theoretical values of OPG (*bold line*), poly(PEG)-OPG (*dotted line*), PEG0.5k-OPG (dashed line) and PEG5k-OPG (*solid line*) generated by Eq. 1. Results are expressed as the mean ± S.D. for at least six individual determinations. The inset shows the IC_{50} values calculated by following Eq. 1. The IC_{50} values of each treatment group were compared by Tukey's test ($p < 0.05$). *, significant difference from PEG0.5k-OPG.

the radioactivity in the bone marrow, liver and spleen retained until 168 h.

The metabolite profiles of ^{14}C-poly(PEG)-OPG in the serum and bone marrow obtained at 3 h post-dose were also analyzed by SE-HPLC and AMS detection (Fig. 7). The chromatogram of ^{14}C-poly(PEG)-OPG in the serum indicated that approximately 88% of total radioactivity was observed at a retention time of 7 min (Fig. 7b), corresponding to the unchanged form of ^{14}C-poly(PEG)-OPG as shown in that of the dosing solution (Fig. 7a). On the other hand, the chromatogram of ^{14}C-poly(PEG)-OPG extracted from the bone marrow showed broad double peaks at 6 and 10 min (Fig. 7c), suggesting that the majority of radioactivity in the bone marrow was derived from the degraded form of ^{14}C-poly(PEG)-OPG.

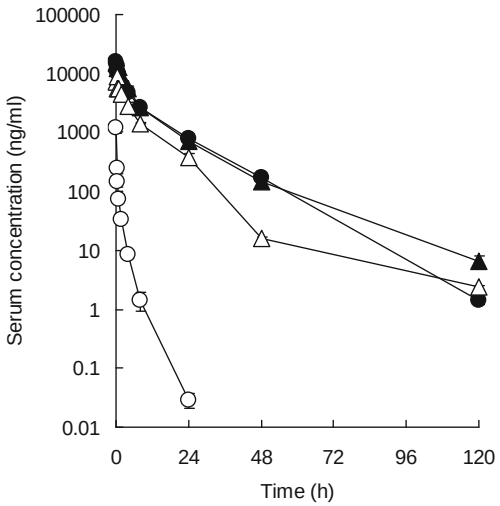

Fig. 4 Serum concentration-time profiles of OPG and PEG-OPG derivatives after intravenous administration (0.3 mg/kg) to OVX rats. Serum concentrations of OPG (*open circle*), poly(PEG)-OPG (*closed circle*), PEG0.5k-OPG (*closed triangle*) and PEG5k-OPG (*open triangle*) were determined by ELISA. Results are expressed as the mean ± S.D. of four rats.

Comparison of Tissue Distribution of ^{125}I-poly(PEG)-OPG with ^{125}I-PEG5k-OPG by Quantitative Whole-Body Autoradioluminography

Tissue distribution of ^{125}I-poly(PEG)-OPG was quantitatively compared with that of ^{125}I-PEG5k-OPG after intravenous administration (0.5 μg/kg) to OVX rats by autoradioluminography. Representative luminograms of ^{125}I-poly(PEG)-OPG and ^{125}I-PEG5k-OPG at 3 h post-dose are shown in Fig. 8a and b, respectively. The radioactivity level was the highest in the bone marrow for both ^{125}I-poly(PEG)-OPG and ^{125}I-PEG5k-OPG, but the bone marrow distribution of ^{125}I-poly(PEG)-OPG was significantly higher than that of ^{125}I-PEG5k-OPG. In the case of ^{125}I-poly(PEG)-OPG, the radioactivity level in the bone marrow was 4.0-fold, 4.5-fold and 2.6-fold higher than those in the liver, adrenal and blood, respectively (Fig. 8c). On the other hand, in ^{125}I-PEG5k-OPG-treated rats, the bone marrow distribution of the radioactivity was slightly higher than those in the liver (1.3-fold), adrenal (1.6-fold) and blood (1.2-fold).

Investigation of Dose-Dependent Pharmacokinetics of Poly(PEG)-OPG

To evaluate the possible non-linearity in pharmacokinetics of poly(PEG)-OPG, the dose-normalized serum concentration-

Table I Pharmacokinetic Parameters of OPG and PEG-OPG Derivatives after Intravenous Administration at a dose of 0.3 mg/kg to OVX Rats

Protein	Half-life (h)	AUC (μg·h/ml)	CL (ml/h/kg)	MRT (h)	Vdss (ml/kg)
OPG	2.54 ± 0.11	0.507 ± 0.070	601 ± 86	0.847 ± 0.036	509 ± 78
Poly(PEG)-OPG	10.5 ± 0.3[a, b, c]	90.4 ± 4.4[a, b, c]	3.32 ± 0.16[a]	11.7 ± 0.5[a, b, c]	38.8 ± 1.5[a]
PEG0.5k-OPG	14.6 ± 0.5[a]	97.8 ± 5.2[a]	3.07 ± 0.16[a]	10.6 ± 0.4[a]	32.6 ± 1.6[a]
PEG5k-OPG	11.6 ± 0.2[a, b]	46.9 ± 1.3[a, b]	6.40 ± 0.18[a]	8.48 ± 0.61[a, b]	54.3 ± 4.0[a]

AUC the area under the serum concentration-time curve; *CL* the total body clearance; *MRT* the mean residence time; *Vdss* the volume of distribution at steady state. Results are expressed as the mean ± S.D. of four rats. The parameters of each treatment group were compared by Tukey's test ($p < 0.05$)

[a] significant difference from OPG

[b] significant difference from PEG0.5k-OPG

[c] significant difference from PEG5k-OPG

time profiles of poly(PEG)-OPG after intravenous administration to OVX rats at doses of 0.5 μg/kg and 0.3 mg/kg were examined (Fig. 9a). As shown in Table II, CL and Vdss significantly decreased and half-life at terminal phase significantly increased with the increase of dose, indicating that the non-linear process was involved in the pharmacokinetics of poly(PEG)-OPG.

For tissue distribution, the effect of excess non-radiolabeled poly(PEG)-OPG (0.3 mg/kg) on the tissue distribution of ^{14}C-poly(PEG)-OPG (0.5 μg/kg) was evaluated in OVX rats at 3 h post-dose (Fig. 9b). The co-administration of excess non-radiolabeled poly(PEG)-OPG dramatically reduced the bone marrow distribution of ^{14}C-poly(PEG)-OPG to about 25% of that in the control rats, suggesting that the uptake of ^{14}C-poly (PEG)-OPG into the bone marrow would be at least partly mediated by some saturable processes. The serum level had significantly increased, which coincided with the results shown in Fig. 9a. However, no significant difference was observed for the hepatic distribution between the two groups.

DISCUSSION

To improve the *in vivo* pharmacological effect of OPG, several PEG-OPG derivatives were synthesized and examined in the present study. It is known that PEG size can affect the pharmacokinetic properties and the biological activities of PEGylated proteins (14,26,27). In the present study, therefore, linear PEG0.5k-OPG and linear PEG5k-OPG were compared with poly(PEG)-OPG, because poly (PEG) is a comb-Shaped PEG (total M_w ca. 5 kDa) having some linear 0.5 kDa PEG chains. In our preliminary study,

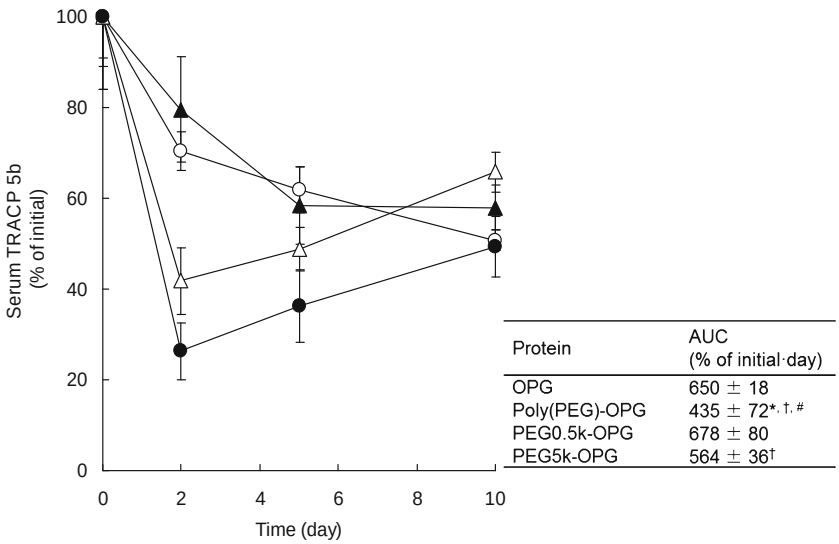

Fig. 5 Serum TRACP 5b level-time profiles (% of initial) after intravenous administration of OPG and PEG-OPG derivatives (0.3 mg/kg). Serum TRACP 5b levels in the rats treated with OPG (open circle), poly(PEG)-OPG (*closed circle*), PEG0.5k-OPG (*closed triangle*) or PEG5k-OPG (open triangle) were determined using a TRACP 5b ELISA kit. The serum TRACP 5b levels were expressed as a percentage of the level on Day 0 (% of initial) in each treatment group. Results are expressed as the mean ± S.D. of five rats. The inset shows the AUC of TRACP 5b levels calculated by following the trapezoidal rule. The AUC of each treatment group were compared by Tukey's test ($p < 0.05$). *, significant difference from OPG; †, significant difference from PEG0.5k-OPG; #, significant difference from PEG5k-OPG.

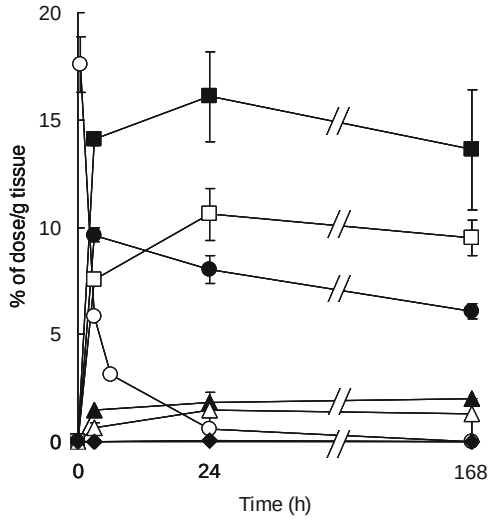

Fig. 6 Tissue distribution of radioactivity after intravenous administration of ^{14}C-poly(PEG)-OPG (0.5 μg/kg) to OVX rats. The radioactivity associated in the bone marrow (closed square), spleen (*open square*), liver (*closed circle*), serum (*open circle*), kidney (*closed triangle*), bone (*open triangle*) and muscle (*closed diamond*) was determined by AMS and normalized with the weight (g) of each organ or the serum sample collected. The results, % of dose per gram in each organ, are expressed as the mean ± S.D. of three rats.

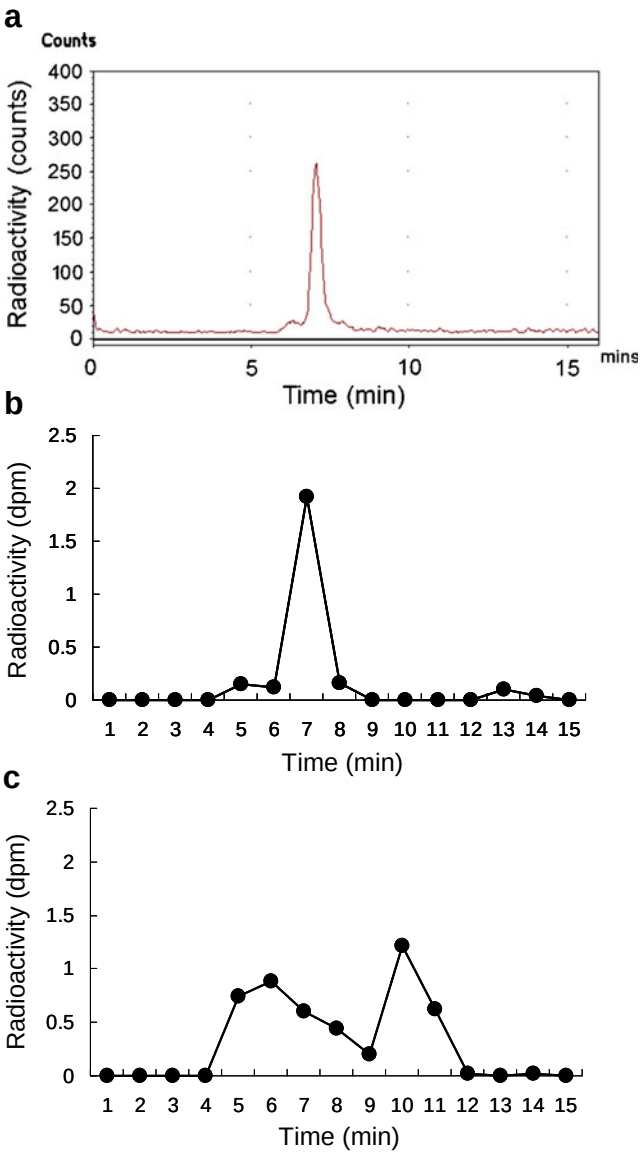

Fig. 7 Typical profiles of degradation of ^{14}C-poly(PEG)-OPG in the serum and bone marrow. (**a**) SE-HPLC-radiochromatogram of ^{14}C-poly(PEG)-OPG dosing solution: SE-HPLC-AMS chromatograms of ^{14}C-poly(PEG)-OPG in (**b**) serum and (**c**) bone marrow. Serum and bone marrow were collected at 3 h after intravenous administration of ^{14}C-poly(PEG)-OPG (0.5 μg/kg) to OVX rats. The radioactivity of each fraction was determined by AMS.

when OPG was conjugated with fewer molar of linear PEG5k than that in the present study (total Mw was similar to that of poly(PEG)-OPG) to eliminate the effect of molecular weight difference. However, the conjugate showed little *in vivo* pharmacological activity due to the short residence time in systemic circulation which was no more than 5-fold higher than that of unmodified OPG. The importance of the present study was to find out PEG-OPG derivatives showing the good bone marrow delivery of OPG and to show the effects of the polymer structure and reaction manner of poly(PEG) on PEGylation domain of OPG. Thus, OPG was conjugated with a large excess of each linear PEG and poly(PEG) and the derivatives showing the residence time in systemic circulation similar to that of poly(PEG)-OPG were obtained.

The biological activity of OPG depends on the specific binding to RANKL (4–7) via the receptor binding domain existing in the N-terminal region of OPG (1,33). A heparin-binding domain in the C-terminal region of OPG, which is lysine-rich and highly-basic, has no precise effect on the receptor binding of OPG (32). In the present study, poly (PEG)-OPG showed the extended *in vivo* half-life and AUC compared with unmodified OPG, which were found to be comparable to those of linear PEG-OPG derivatives (Fig. 4 and Table I), although poly(PEG) molecules modified OPG in a different manner from linear PEG molecules and the number of poly(PEG) molecules attached to OPG could be much less than that of linear PEG molecules (Fig. 2). The short half-life of OPG from the systemic circulation is attributed to the interaction with the liver via the heparin-binding domain of OPG (12), although basic proteins and peptides are known to be rapidly distributed to the tissues, resulting in their rapid elimination (34). In addition, DS5-OPG in which the heparin-binding domain of OPG was masked with dextran sulfate, revealed a significantly longer *in vivo* half-life than OPG (12). These reports clearly indicate that the interaction with liver via heparin-binding domain of OPG is important for OPG derivatives to eliminate from systemic circulation, therefore, the modification with poly (PEG) or linear PEG would effectively mask the heparin-binding domain at similar levels.

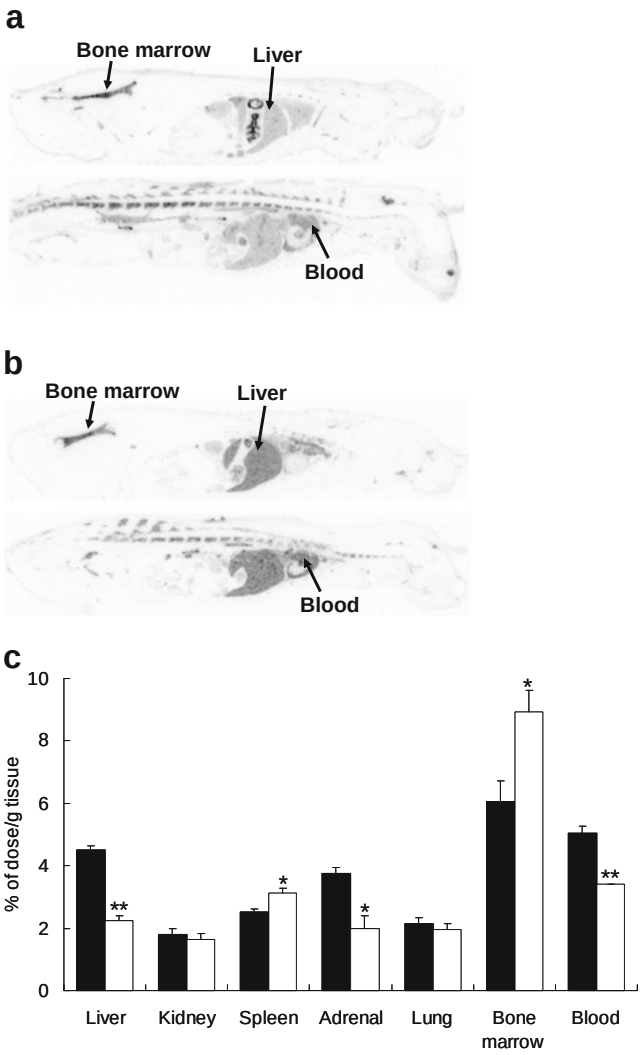

Fig. 8 Whole-body tissue distribution of radioactivity at 3 h after intravenous administration of ^{125}I-PEG-OPG derivatives to OVX rats. (**a**) ^{125}I-poly(PEG)-OPG (0.5 μg/kg). (**b**) ^{125}I-PEG5k-OPG (0.5 μg/kg). (**c**) The tissue distribution (% of dose/g tissue) of ^{125}I-poly(PEG)-OPG (*open column*) and ^{125}I-PEG5k-OPG (*closed column*), which were calculated from the whole-body autoradioluminograms using a Bio Imaging Analyzer. Results are expressed as the mean with the vertical bar showing S.D. for three rats. The tissue distribution of ^{125}I-poly(PEG)-OPG was compared with that of ^{125}I-PEG5k-OPG by Student's *t*-test (*$p < 0.01$, **$p < 0.001$).

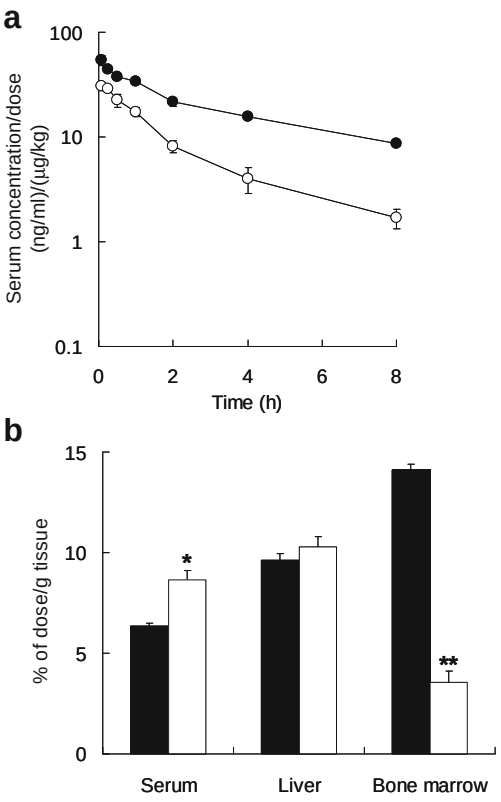

Fig. 9 Dose-dependent pharmacokinetics of poly(PEG)-OPG. (**a**) Dose-normalized serum concentrations-time profiles of poly(PEG)-OPG after intravenous administration at doses of 0.5 μg/kg (*open circle*) and 0.3 mg/kg (*closed circle*) to OVX rats. Serum concentrations were determined by ELISA. Results are expressed as the mean ± S.D. of four rats. (**b**) Effect of excess non-radiolabeled poly(PEG)-OPG on the tissue distribution of ^{14}C-poly(PEG)-OPG. ^{14}C-poly(PEG)-OPG (0.5 μg/kg) was intravenously co-administered with (*open column*) or without (*closed column*) non-radiolabeled poly(PEG)-OPG (0.3 mg/kg) to OVX rats. The radioactivity concentrations of the bone marrow, liver and serum at 3 h post-dose were determined by AMS. Results are expressed as the mean with the vertical bar showing S.D. of three rats. The tissue distribution in control rats was compared with that in the rats treated with excess non-labeled poly(PEG)-OPG by Student's *t*-test (*$p < 0.01$, **$p < 0.001$).

On the other hand, poly(PEG) modification could substantially preserve the binding affinity of OPG to RANKL (Fig. 3), whereas linear PEG modification severely reduced the receptor binding affinity by less than one-fifth compared with poly(PEG)-OPG. In addition, poly(PEG)-OPG showed the highest *in vivo* potency among the three PEG-OPG derivatives examined (Fig. 5), although *in vivo* half-life and AUC of poly(PEG)-OPG were comparable to those of linear PEG-OPG derivatives (Fig. 4 and Table I). These results also support that poly(PEG) modification has an advantage over the linear PEG modification, although the exact conjugation sites of poly(PEG) remains to be clarified.

Since intravenously injected OPG was mainly distributed to the liver, where OPG concentration was about 7-fold higher than that in the bone marrow (12), it was clearly indicated that poly(PEG) modification could successfully increase the bone marrow distribution of OPG, which was the highest among the tissue examined (Fig. 6). A greater part of the radioactivity distributed into the bone marrow existed as degraded forms of ^{14}C-poly(PEG)-OPG at 3 h post-dose (Fig. 7c), while almost all of ^{14}C-poly(PEG)-OPG existed as an intact form in the serum (Fig. 7b). Furthermore, the bone marrow distribution of ^{14}C-poly(PEG)-OPG was remarkably reduced by co-administration of excess non-radiolabeled poly(PEG)-OPG (Fig. 9b). These results suggest the RANKL-mediated distribution and internalization of poly(PEG)-OPG into the bone marrow cells, followed by degradation in lysosomes and proteasomes, which was reported in the case of OPG (33).

Table II Pharmacokinetic Parameters of Poly(PEG)-OPG After Intravenous Administration at Doses of 0.5 μg/kg and 0.3 mg/kg to OVX Rats

Dose	Half-life (h)	AUC/dose (ng·h/ml)/(μg/kg)	CL (ml/h/kg)	MRT (h)	Vdss (ml/kg)
0.5 μg/kg	2.70 ± 0.12	66.6 ± 9.7	15.2 ± 2.0	2.93 ± 0.23	44.3 ± 3.1
0.3 mg/kg	4.57 ± 0.39*	211 ± 8*	4.75 ± 0.18*	5.94 ± 0.46*	28.2 ± 1.8*

AUC the area under the serum concentration-time curve; *CL* the total body clearance; *MRT* the mean residence time; *Vdss* the volume of distribution at steady state. Results are expressed as the means ± S.D. of four rats. The parameters of 0.3 mg/kg were compared with those of 0.5 μg/kg by Student's *t*-test (* $p < 0.05$)

In whole-body autoradioluminography (Fig. 8), ^{125}I-poly(PEG)-OPG showed significantly higher bone marrow distribution, better bone marrow-to-blood ratio and bone marrow-to-liver ratio than those of ^{125}I-PEG5k-OPG, suggesting that ^{125}I-poly(PEG)-OPG has a promising ability for the specific distribution to the target tissue compared with linear PEG5k-OPG. For evaluation of tissue distribution of poly(PEG)-OPG, ^{14}C-labeled poly(PEG)-OPG in which the polymer was ^{14}C-labeled, and ^{125}I-labeled poly(PEG)-OPG in which the protein was ^{125}I-labeled, were used in the present study. Since the detection method was also different, the absolute values of the tissue concentrations of ^{14}C-poly(PEG)-OPG could not completely be consistent with those of ^{125}I-poly(PEG)-OPG (Figs. 6 and 8). However, the descending order of the tissue concentration of the radioactivity was almost consistent between ^{14}C-poly(PEG)-OPG and ^{125}I-poly(PEG)-OPG (bone marrow > liver ≈ spleen ≈ blood > kidney).

Poly(PEG)-OPG showed non-linear pharmacokinetic properties (Fig. 9a and Table II) , which may be attributed to the saturable uptake process by the bone marrow due to the following reasons. The average weight of the whole bone marrow of rats used in this study was estimated to be 3.1 g based on the report that the total bone marrow weight was 4 g/200 g rat (35). Therefore, the radioactivity in the whole bone marrow and whole liver were calculated to be 44% and 35% of dose at 3 h post-dose of ^{14}C-poly(PEG)-OPG (0.5 μg/kg), respectively, based on the results shown in Fig. 6. This estimation suggests that the uptake amount to the bone marrow was larger than that to the liver, and that about half of the total uptake clearance of ^{14}C-poly(PEG)-OPG could be attributed to the uptake clearance to the bone marrow, which would be saturable while the hepatic uptake might not be saturable (Figs. 3 and 9b). It was also reported that saturable bone marrow uptake by the specific receptor could substantially contribute to the non-linear elimination of nartograstim which is the recombinant human granulocyte colony-stimulating factor derivative (36).

A heparin-binding domain in OPG has high-density basic amino acids such as lysine exposed to solvent compared with other domains (32). Since the carbonyl carbons of the neighboring maleyl amide bond could be vulnerable to a nucleophilic attack by primary amines, this could lead to binding to the primary amines and leaving of the amino groups from the maleyl amide bond (37). In addition, it was confirmed that ε-maleyl-lysine was formed when maleamic acid was incubated with L-lysine overnight at 37°C, pH4.7 (data not shown). Thus, the carbonyl carbons in maleyl amide bond of poly(PEG) could bind to the ε-amino group of L-lysine in OPG via the nucleophilic substitution to form ε-maleyl-lysine conjugation. Furthermore, because poly(PEG) has a number of maleamic acid units in which there are negatively-charged carboxyl groups and reactive maleyl amide groups, poly(PEG) could easily approach the heparin-binding domain with electrostatic interaction, but is not likely to electrostatically bind other domains in OPG. In addition, since the reactivity of maleamic acid units of poly(PEG) is quite mild (37) and the structure of poly(PEG) is sterically-bulky, lysine residues beyond the surface could not be easily modified by poly(PEG). Therefore, fewer numbers of poly(PEG) molecules could modify OPG at the heparin-binding domain compared with linear PEG molecules. These reasons described above would have resulted in that poly(PEG) could effectively cover the heparin-binding domain with fewer numbers of poly(PEG) molecules (Fig. 4 and Table I) and preserve the binding affinity for RANKL (Fig. 3). On the other hand, linear PEG-NHS molecules could modify more numbers of lysine residues prevailing throughout OPG, because N-hydroxysuccinimide in linear PEG-NHS molecules have extremely high chemical reactivity (38), and linear PEG is not sterically-bulky compared with poly(PEG). Therefore, the numbers of linear PEG molecules attached to OPG were much larger than those of poly(PEG) molecules. These would be reasons why linear PEG molecules are likely to modify the receptor binding domain, compared with poly(PEG) molecules, resulting in the drastic reduction of the biological activity of linear PEG-OPG derivatives (Figs. 3 and 5).

Although it would be a challenging goal to site-specifically modify with PEG, any preferable amino acids in a protein, poly(PEG) could preferentially modify a heparin-binding domain of OPG without application of site-directed mutagenesis of a protein in the present study. Since many bioactive proteins such as the vascular endothelial growth factor (39) and basic fibroblast growth factor (40) have a heparin-binding domain having the motifs of which the majority have the consensus amino-acid sequences (41), similar to the heparin-

binding domain of OPG (1,3), poly(PEG) has the potential to be applicable to other bioactive proteins to modify the heparin-binding domain, although further research would be necessary for it.

In conclusion, a novel comb-shaped poly(PEG) modification of OPG could effectively mask the heparin-binding domain of OPG, leading to the prolongation of the residence time in the systemic circulation, and could preserve the binding affinity for RANKL, resulting in the bone-marrow specific delivery and the enhancement of the *in vivo* pharmacological efficacy. The present study clearly indicated that poly(PEG) modification would be the better option for optimizing a therapeutic potential of OPG.

REFERENCES

1. Simonet WS, Lacey DL, Dunstan CR, Kelley M, Chang MS, Lüthy R, *et al.* Osteoprotegerin: a novel secreted protein involved in the regulation of bone density. Cell. 1997;89(2):309–19.
2. Tsuda E, Goto M, Mochizuki S, Yano K, Kobayashi F, Morinaga T, *et al.* Isolation of a novel cytokine from human fibroblasts that specifically inhibits osteoclastogenesis. Biochem Biophys Res Commun. 1997;234(1):137–42.
3. Yamaguchi K, Kinosaki M, Goto M, Kobayashi F, Tsuda E, Morinaga T, *et al.* Characterization of structural domains of human osteoclastogenesis inhibitory factor. J Biol Chem. 1998;273 (9):5117–23.
4. Lacey DL, Timms E, Tan HL, Kelley MJ, Dunstan CR, Burgess T, *et al.* Osteoprotegerin ligand is a cytokine that regulates osteoclast differentiation and activation. Cell. 1998;93(2):165–76.
5. Yasuda H, Shima N, Nakagawa N, Yamaguchi K, Kinosaki M, Mochizuki S, *et al.* Osteoclast differentiation factor is a ligand for osteoprotegerin/osteoclastogenesis-inhibitory factor and is identical to TRANCE/RANKL. Proc Natl Acad Sci USA. 1998;95 (7):3597–602.
6. Yasuda H, Shima N, Nakagawa N, Mochizuki SI, Yano K, Fujise N, *et al.* Identity of osteoclastogenesis inhibitory factor (OCIF) and osteoprotegerin (OPG): a mechanism by which OPG/OCIF inhibits osteoclastogenesis *in vitro*. Endocrinology. 1998;139(3):1329–37.
7. Hsu H, Lacey DL, Dunstan CR, Solovyev I, Colombero A, Timms E, *et al.* Tumor necrosis factor receptor family member RANK mediates osteoclast differentiation and activation induced by osteoprotegerin ligand. Proc Natl Acad Sci USA. 1999;96(7):3540–5.
8. Morony S, Capparelli C, Lee R, Shimamoto G, Boone T, Lacey DL, *et al.* A chimeric form of osteoprotegerin inhibits hypercalcemia and bone resorption induced by IL-1beta, TNF-alpha, PTH, PTHrP, and 1, 25(OH)2D3. J Bone Miner Res. 1999;14(9):1478–85.
9. Capparelli C, Kostenuik PJ, Morony S, Starnes C, Weimann B, Van G, *et al.* Osteoprotegerin prevents and reverses hypercalcemia in a murine model of humoral hypercalcemia of malignancy. Cancer Res. 2000;60(4):783–7.
10. Kostenuik PJ, Capparelli C, Morony S, Adamu S, Shimamoto G, Shen V, *et al.* OPG and PTH-(1-34) have additive effects on bone density and mechanical strength in osteopenic ovariectomized rats. Endocrinology. 2001;142(10):4295–404.
11. Bekker PJ, Holloway D, Nakanishi A, Arrighi M, Leese PT, Dunstan CR. The effect of a single dose of osteoprotegerin in postmenopausal women. J Bone Miner Res. 2001;16(2):348–60.
12. Miyaji Y, Kurihara A, Kamiyama E, Shiiki T, Kawai K, Okazaki O. Pharmacokinetics and disposition of recombinant human osteoprotegerin (rhOPG) after intravenous administration in female Fischer rats. Xenobiotica. 2009;39(2):113–24.
13. Roberts MJ, Bentley MD, Harris JM. Chemistry for peptide and protein PEGylation. Adv Drug Deliv Rev. 2002;54(4):459–76.
14. Youn YS, Kwon MJ, Na DH, Chae SY, Lee S, Lee KC. Improved intrapulmonary delivery of site-specific PEGylated salmon calcitonin: optimization by PEG size selection. J Control Release. 2008;125(1):68–75.
15. Abuchowski A, McCoy JR, Palczuk NC, van Es T, Davis FF. Effect of covalent attachment of polyethylene glycol on immunogenicity and circulating life of bovine liver catalase. J Biol Chem. 1977;252 (11):3582–6.
16. Harris JM, Chess RB. Effect of pegylation on pharmaceuticals. Nat Rev Drug Discov. 2003;2(3):214–21.
17. Caliceti P, Veronese FM. Pharmacokinetic and biodistribution properties of poly(ethylene glycol)-protein conjugates. Adv Drug Deliv Rev. 2003;55(10):1261–77.
18. Kim WJ, Yockman JW, Jeong JH, Christensen LV, Lee M, Kim YH, *et al.* Anti-angiogenic inhibition of tumor growth by systemic delivery of PEI-g-PEG-RGD/pCMV-sFlt-1 complexes in tumor-bearing mice. J Control Release. 2006;114(3):381–8.
19. Veronese FM, Pasut G. PEGylation, successful approach to drug delivery. Drug Discov Today. 2005;10(21):1451–8.
20. Ryan SM, Mantovani G, Wang X, Haddleton DM, Brayden DJ. Advances in PEGylation of important biotech molecules: delivery aspects. Expert Opin Drug Deliv. 2008;5(4):371–83.
21. Bailon P, Palleroni A, Schaffer CA, Spence CL, Fung WJ, Porter JE, *et al.* Rational design of a potent, long-lasting form of interferon: a 40 kDa branched polyethylene glycol-conjugated interferon alpha-2a for the treatment of hepatitis C. Bioconjug Chem. 2001;12(2):195–202.
22. Wang YS, Youngster S, Bausch J, Zhang R, McNemar C, Wyss DF. Identification of the major positional isomer of pegylated interferon alpha-2b. Biochemistry. 2000;39(35):10634–40.
23. Saito-Yabe M, Kasuya Y, Yoshigae Y, Yamamura N, Suzuki Y, Fukuda N, *et al.* PEGylation of osteoprotegerin/osteoclastogenesis inhibitory factor (OPG/OCIF) results in decreased uptake into rats and human liver. J Pharm Pharmacol. 2010;62(8):985–94.
24. Ryan SM, Wang X, Mantovani G, Sayers CT, Haddleton DM, Brayden DJ. Conjugation of salmon calcitonin to a combed-shaped end functionalized poly(poly(ethylene glycol) methyl ether methacrylate) yields a bioactive stable conjugate. J Control Release. 2009;135(1):51–9.
25. Kodera Y, Sekine T, Yasukohchi T, Kiriu Y, Hiroto M, Matsushima A, *et al.* Stabilization of L-asparaginase modified with comb-shaped poly(ethylene glycol) derivatives, *in vivo* and *in vitro*. Bioconjug Chem. 1994;5(4):283–6.
26. Uchio T, Baudys M, Liu F, Song SC, Kim SW. Site-specific insulin conjugates with enhanced stability and extended action profile. Adv Drug Deliv Rev. 1999;35(2–3):289–306.
27. Bell SJ, Fam CM, Chlipala EA, Carlson SJ, Lee JI, Rosendahl MS, *et al.* Enhanced circulating half-life and antitumor activity of a site-specific pegylated interferon-alpha protein therapeutic. Bioconjug Chem. 2008;19(1):299–305.
28. Mochizuki K, Inoue T. Effect of salmon calcitonin on experimental osteoporosis induced by ovariectomy and low-calcium diet in the rat. J Bone Miner Metab. 2000;18(4):194–207.
29. Alatalo SL, Peng Z, Janckila AJ, Kaija H, Vihko P, Vaananen HK, *et al.* A novel immunoassay for the determination of tartrate-resistant acid phosphatase 5b from rat serum. J Bone Miner Res. 2003;18(1):134–9.
30. Kitagawa H, Masuzawa T, Nakamura T, Matsumoto E. A batch preparation method for graphite targets with low background for AMS 14C measurements. Radiocarbon. 1993;35(3):295–300.
31. Miyaji Y, Ishizuka T, Kawai K, Hamabe Y, Miyaoka T, Oh-hara T, *et al.* Use of an intravenous microdose of 14C-labeled drug and

accelerator mass spectrometry to measure absolute oral bioavailability in dogs; cross-comparison of assay methods by accelerator mass spectrometry and liquid chromatography-tandem mass spectrometry. Drug Metab Pharmacokinet. 2009;24(2):130–8.
32. Tomoyasu A, Goto M, Fujise N, Mochizuki S, Yasuda H, Morinaga T, *et al.* Characterization of monomeric and homodimeric forms of osteoclastogenesis inhibitory factor. Biochem Biophys Res Commun. 1998;245(2):382–7.
33. Tat SK, Padrines M, Theoleyre S, Couillaud-Battaglia S, Heymann D, Redini F, *et al.* OPG/membranous-RANKL complex is internalized via the clathrin pathway before a lysosomal and a proteasomal degradation. Bone. 2006;39(4):706–15.
34. Miyaji Y, Walter S, Chen L, Kurihara A, Ishizuka T, Saito M, *et al.* Distribution of KAI-9803, a novel δPKC inhibitor, after intravenous administration to rats. Drug Metab Dispos. 2011;39 (10):1946–53.
35. Dedrick RL, Zaharko DS, Lutz RJ. Transport and binding of methotrexate *in vivo*. J Pharm Sci. 1973;62(6):882–90.
36. Kuwabara T, Uchimura T, Takai K, Kobayashi H, Kobayashi S, Sugiyama Y. Saturable uptake of a recombinant human granulocyte colony-stimulating factor derivative, nartograstim, by the bone marrow and spleen of rats *in vivo*. J Pharmacol Exp Ther. 1995;273(3):1114–22.
37. Butler PJ, Harris JI, Hartley BS, Lebeman R. The use of maleic anhydride for the reversible blocking of amino groups in polypeptide chains. Biochem J. 1969;112(5):679–89.
38. Nojima Y, Iguchi K, Suzuki Y, Sato A. The pH-dependent formation of PEGylated bovine lactoferrin by branched polyethylene glycol (PEG)-N-hydroxysuccinimide (NHS) active esters. Biol Pharm Bull. 2009;32(3):523–6.
39. Gitay-Goren H, Soker S, Vlodavsky I, Neufeld G. The binding of vascular endothelial growth factor to its receptors is dependent on cell surface-associated heparin-like molecules. J Biol Chem. 1992;267(9):6093–8.
40. Sakaguchi K, Yanagishita M, Takeuchi Y, Aurbach GD. Identification of heparan sulfate proteoglycan as a high affinity receptor for acidic fibroblast growth factor (aFGF) in a parathyroid cell line. J Biol Chem. 1991;266(11):7270–8.
41. El-Sheikh A, Liu C, Huang H, Edgington TS. A novel vascular endothelial growth factor heparin-binding domain substructure binds to glycosaminoglycans *in vivo* and localizes to tumor microvascular endothelium. Cancer Res. 2002;62(23):7118–23.